

Synthesis and Helicate Formation of a New Family of BINOL-Based Bis(bipyridine) Ligands

Jens Bunzen,[†] Torsten Bruhn,[#] Gerhard Bringmann,^{*,#} and Arne Lützen^{*,†}

Kekulé-Institute of Organic Chemistry and Biochemistry, University of Bonn, Gerhard-Domagk-Strasse 1, D-53121 Bonn, Germany, and Institute of Organic Chemistry, University of Würzburg, Am Hubland, D-97074 Würzburg, Germany

Received October 2, 2008; E-mail: bringmann@chemie.uni-wuerzburg.de; arne.luetzen@uni-bonn.de

Abstract: A new family of BINOL-based bis(bipyridine) ligands **1–3** (BINOL = 2,2'-dihydroxy-1,1'-binaphthyl) was prepared in enantiomerically pure form. Whereas the coordination of zinc(II) ions to these ligands did not result in the selective formation of a specific metallosupramolecular aggregate, **1–3** were found to undergo highly diastereoselective self-assembly to D_2 -symmetric dinuclear double-stranded helicates upon coordination to silver(I) and copper(I) ions and to D_3 -symmetric dinuclear triple-stranded helicates upon coordination to iron(II) as demonstrated by mass spectrometry and by NMR and CD spectroscopy in combination with quantum chemical calculations.

Introduction

The formation of supramolecular aggregates by self-assembly is a widely accepted method to build up sophisticated molecular architectures.¹ In this respect complexes bearing cavities large enough to encapsulate guest molecules are of special interest because they exhibit a number of exciting properties such as the possibilities to stabilize and study reactive molecules or to act as nanoreaction vessels that permit formation of reaction products which are not obtainable in bulk solutions because of the unique confined environments offered by the cavities.^{2,3} Besides a certain size and chemical nature (provided by eventually available functional groups pointing inside the cavity), chirality is a highly desired feature in order to achieve stereoselectivity in host–guest chemistry and further processes related to the recognition event. Helicates are chiral objects that can provide chiral cavities.⁴ In this respect, such metallo-supramolecular aggregates are highly attractive because they can be produced in a stereocontrolled manner through diastereoselective self-assembly from chiral ligands as demonstrated in many beautiful examples in recent years.^{4–9}

We have also reported on some dissymmetrical ligands that can be used to prepare helicates with different cavity sizes and chemical properties in a diastereoselective fashion.^{10–13} One of these is a BINOL-based bis(bipyridine) ligand in which the bipyridine metal binding sites are connected to the 3- and 3'-

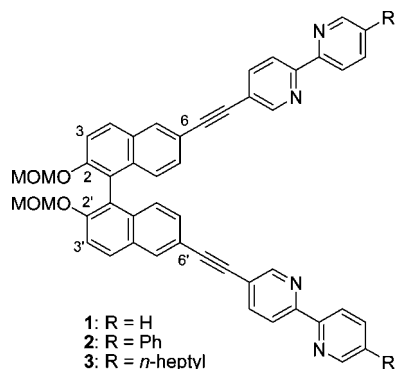
positions of the BINOL core via ethynylene spacers.¹⁰ This ligand undergoes stereoselective self-assembly to discrete enantiomerically pure double- and triple-stranded helicates upon coordination to late transition metal ions such as copper(I), silver(I), iron(II), or zinc(II) ions. Now, we have extended this approach by modifying the ligand design: In our previous work the substitution pattern of the BINOL part positioned the (protected) hydroxyl functions inside the cavity of the assembly. For the new class of ligands **1–3** (Scheme 1) reported here, we changed the substitution pattern of the BINOL from 3,3' to 6,6', to investigate how this change influences the self-assembly

- (3) Self-assembly by metal coordination:(a) Leininger, S.; Olenyuk, B.; Stang, P. J. *Chem. Rev.* **2000**, *100*, 853–907. (b) Swiegers, G. F.; Malefetse, T. J. *Chem. Rev.* **2000**, *100*, 3483–3537. (c) Holliday, B. J.; Mirkin, C. A. *Angew. Chem., Int. Ed.* **2001**, *40*, 2022–2043. (d) Seidel, S. R.; Stang, P. J. *Acc. Chem. Res.* **2002**, *35*, 972–983. (e) Würthner, F.; You, C.-C.; Saha-Möller, C. R. *Chem. Soc. Rev.* **2004**, *33*, 133–146. (f) Yeh, R. M.; Davis, A. V.; Raymond, K. N. In *Comprehensive Coordination Chemistry II*; Meyer, T. J., Ed.; Elsevier: Oxford, 2004; pp 327–355. (g) Schmittel, M.; Kalsani, V. *Top. Curr. Chem.* **2005**, *245*, 1–53. (h) Fiedler, D.; Leung, D. H.; Bergman, R. G.; Raymond, K. N. *Acc. Chem. Res.* **2005**, *38*, 349–358. (i) Fujita, M.; Tominaga, M.; Hori, A.; Therrien, B. *Acc. Chem. Res.* **2005**, *38*, 369–378. (j) Sianneschi, N. C.; Masar, M. S.; Mirkin, C. A. *Acc. Chem. Res.* **2005**, *38*, 825–837. (k) Arrijs, C. H. M.; van Klink, G. P. M.; van Koten, G. J. *Chem. Soc., Dalton Trans.* **2006**, 308–327. (l) Maurizot, V.; Yoshizawa, M.; Kawano, M.; Fujita, M. *J. Chem. Soc., Dalton Trans.* **2006**, 2750–2756. (m) Tominaga, M.; Fujita, M. *Bull. Chem. Soc. Jpn.* **2007**, *80*, 1473–1482. (n) Chen, C.-L.; Zhang, J.-Y.; Su, C.-Y. *Eur. J. Inorg. Chem.* **2007**, 299, 7–3010. (o) Thomas, J. A. *Chem. Soc. Rev.* **1997**, *36*, 856–868.
- (4) Reviews:(a) Piguet, C.; Bernardinelli, G.; Hopfgartner, G. *Chem. Rev.* **1997**, *97*, 2005–2062. (b) Albrecht, M. *Chem. Soc. Rev.* **1998**, *27*, 281–288. (c) Knof, U.; von Zelewsky, A. *Angew. Chem., Int. Ed.* **1999**, *38*, 303–322. (d) Caulder, D. L.; Raymond, K. N. *J. Chem. Soc., Dalton Trans.* **1999**, 1185–1200. (e) Caulder, D. L.; Raymond, K. N. *Acc. Chem. Res.* **1999**, *32*, 975–982. (f) von Zelewsky, A. *Coord. Chem. Rev.* **1999**, *190–192*, 811–825. (g) von Zelewsky, A.; Mamula, O. *J. Chem. Soc., Dalton Trans.* **2000**, 219–231. (h) Albrecht, M. *Chem.–Eur. J.* **2000**, *6*, 3485–3489. (i) Albrecht, M. *Chem. Rev.* **2001**, *101*, 3457–3497. (j) Bünzli, J.-C. G.; Piguet, C. *Chem. Rev.* **2002**, *102*, 1897–1928. (k) Mamula, O.; von Zelewsky, A. *Coord. Chem. Rev.* **2003**, *242*, 87–95.

[†] University of Bonn.

[#] University of Würzburg.

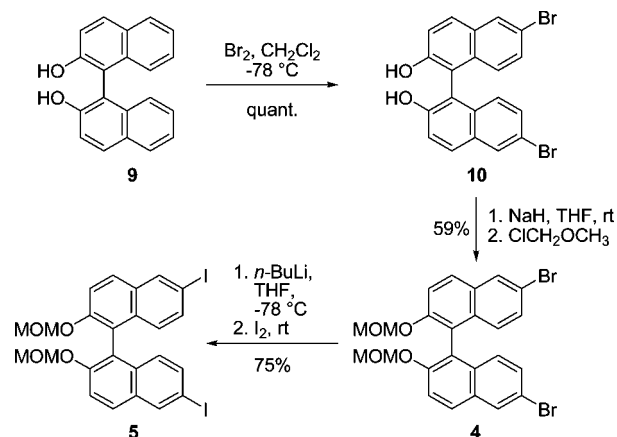
- (1) Some general reviews:(a) Lindsey, J. S. *New J. Chem.* **1991**, *15*, 153–180. (b) Lawrence, D. S.; Jiang, T.; Levett, M. *Chem. Rev.* **1995**, *95*, 2229–2260. (c) Fyfe, M. C. T.; Stoddart, J. F. *Acc. Chem. Res.* **1997**, *30*, 393–401. (d) Greig, L. M.; Philp, D. *Chem. Soc. Rev.* **2001**, *30*, 287–302.
- (2) Self-assembly by hydrogen bonding:(a) Hof, F.; Craig, S. L.; Nuckolls, C.; Rebek, J., Jr. *Angew. Chem., Int. Ed.* **2002**, *41*, 1488–1508. (b) Rebek, J., Jr. *J. Org. Chem.* **2004**, *69*, 2651–2660. (c) Palmer, L. C.; Rebek, J., Jr. *Org. Biomol. Chem.* **2004**, *2*, 3051–3059. (d) Rebek, J., Jr. *Angew. Chem., Int. Ed.* **2005**, *44*, 2068–2078. (e) Scarso, A.; Rebek, J., Jr. *Top. Curr. Chem.* **2006**, *265*, 1–46. (f) Rebek, J., Jr. *Chem. Commun.* **2007**, 2777–2789.

Scheme 1. 6,6'-Substituted BINOL-Based Bis(bipyridine) Ligands 1–3

behavior and to get access to metallo-supramolecular aggregates whose outer surface is equipped with phenolic groups. As compared to the new ligand **1**, the other two ligands, **2** and **3**, contain further hydrocarbon groups in the 5'-position of the bipyridine to provide better solubility of the ligand and its metal complexes.

Results and Discussion

Synthesis. Compounds **1–3** were prepared in a convergent manner by cross-coupling of suitable 6,6'-dihalogenated MOM-

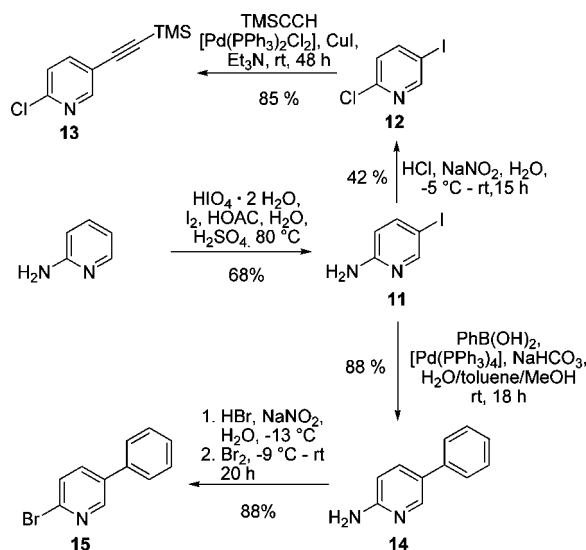
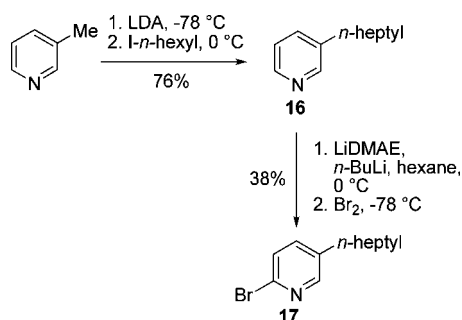
Scheme 2. Synthesis of 6,6'-Dihalogenated BINOL Building Blocks **4** and **5**

protected BINOLs **4** or **5** with the 5-ethynylated 2,2'-bipyridine derivatives **6–8**. BINOLs **4** and **5** were synthesized in four and five steps, respectively, following known procedures starting from commercially available 2-naphthol. Oxidative coupling of naphthol with iron(III) chloride¹⁴ followed by resolution through clathrate formation with *N*-benzylcinchonidinium chloride gave enantiomerically pure (*M*)- and (*P*)-BINOL (**9**).¹⁵ Both enantiomers of **9** were then brominated regioselectively to give (*M*)- and (*P*)-**10**,¹⁶ which were subsequently MOM-protected to give the desired dibrominated building blocks (*M*)- and (*P*)-**4**.¹⁷ In order to deliver an even more reactive building block for the final Sonogashira reaction the bromine atoms were substituted by iodines by lithium–bromine exchange and subsequent quenching with iodine to yield (*M*)- and (*P*)-**5** (Scheme 2).¹⁷

2,2'-Bipyridines **6–8** were prepared from commercially available pyridines (Schemes 3–5). 2-Aminopyridine was iodinated to give 2-amino-5-iodopyridine (**11**) in 68% yield.¹⁸ A first portion of **11** was subjected to a Sandmeyer reaction to give 2-chloro-5-iodopyridine (**12**) in 42% yield.¹⁹ Sonogashira cross-coupling with TMS-protected acetylene using standard conditions furnished the first pyridine building block **13** carrying the ethynyl function.²⁰ By palladium-catalyzed Suzuki reaction with phenylboronic acid, a second portion of **11** was transformed into 2-amino-5-phenylpyridine (**14**) in 88% yield.²¹ Subsequent

- (5) Selected examples of the diastereoselective formation of helicates with 2,2'-bipyridines: (a) Zarges, W.; Hall, J.; Lehn, J.-M.; Bolm, C. *Helv. Chim. Acta* **1991**, *74*, 1843–1852. (b) Mamula, O.; von Zelewsky, A.; Bark, T.; Bernardinelli, G. *Angew. Chem., Int. Ed.* **1999**, *38*, 2945–2948. (c) Mamula, O.; Monlien, F. J.; Porquet, A.; Hopfgartner, G.; Merbach, A. E.; von Zelewsky, A. *Chem.—Eur. J.* **2001**, *7*, 533–539. (d) Mamula, O.; von Zelewsky, A.; Brodard, P.; Schlöpfer, C.-W.; Bernardinelli, G.; Stoeckli-Evans, H. *Chem.—Eur. J.* **2005**, *11*, 3049–3057. (e) Woods, C. R.; Benaglia, M.; Cozzi, F.; Siegel, J. S. *Angew. Chem., Int. Ed.* **1996**, *35*, 1830–1833. (f) Annunziata, R.; Benaglia, M.; Cinquini, M.; Cozzi, F.; Woods, C. R.; Siegel, J. S. *Eur. J. Org. Chem.* **2001**, 173–180. (g) Baum, G.; Constable, E. C.; Fenske, D.; Housecroft, C. E.; Kulke, T. *Chem. Commun.* **1999**, 195–196. (h) Prabaharan, R.; Fletcher, N. C.; Nieuwenhuyzen, M. *J. Chem. Soc., Dalton Trans.* **2002**, 602–608. (i) Prabaharan, R.; Fletcher, N. C. *Inorg. Chim. Acta* **2003**, *355*, 449–453. (j) Telfer, S. G.; Tajima, N.; Kuroda, R. *J. Am. Chem. Soc.* **2004**, *126*, 1408–1418.
- (6) Selected examples of the diastereoselective formation of helicates with ter- and quaterpyridines: (a) Baum, G.; Constable, E. C.; Fenske, D.; Housecroft, E.; Kulke, T.; Neuburger, M.; Zehnder, M. *J. Chem. Soc., Dalton Trans.* **2000**, 945–959. (b) Baum, G.; Constable, E. C.; Fenske, D.; Housecroft, C. E.; Kulke, T. *Chem.—Eur. J.* **1999**, *5*, 1862–1873.
- (7) Selected examples of the diastereoselective formation of helicates with oxazolines and pyridylmethanimines: (a) Provent, C.; Rivara-Minten, E.; Hewage, S.; Brunner, G.; Williams, A. F. *Chem.—Eur. J.* **1999**, *5*, 3487–3494. (b) van Stein, G. C.; van Koten, G.; Vrieze, K.; Brevard, C.; Spek, A. L. *J. Am. Chem. Soc.* **1984**, *106*, 4486–4492. (c) Masood, M. A.; Enemark, E. J.; Stack, T. D. P. *Angew. Chem., Int. Ed.* **1998**, *37*, 928–931. (d) Amendola, V.; Fabbrizzi, L.; Mangano, C.; Pallavicini, P.; Roboli, E.; Zema, M. *Inorg. Chem.* **2000**, *39*, 5803–5806. (e) Hamblin, J.; Childs, L. J.; Alcock, N. W.; Hannon, M. J. *J. Chem. Soc., Dalton Trans.* **2002**, 164–169. See also ref 5i.
- (8) Selected examples of the diastereoselective formation of helicates with catechols: (a) Kersting, B.; Meyer, M.; Powers, R. E.; Raymond, K. N. *J. Am. Chem. Soc.* **1996**, *118*, 7221–7222. (b) Enemark, E. J.; Stack, T. D. P. *Angew. Chem., Int. Ed.* **1995**, *34*, 996–998. (c) Enemark, E. J.; Stack, T. D. P. *Angew. Chem., Int. Ed.* **1998**, *37*, 932–935. (d) Albrecht, M. *Synlett* **1996**, 565–567. (e) Albrecht, M.; Janser, I.; Fleischhauer, J.; Wang, Y.; Raabe, G.; Fröhlich, R. *Mendeleev Commun.* **2004**, 250–253.
- (9) Selected examples of the diastereoselective formation of helicates with P-donor ligands: (a) Airey, A. L.; Swiegers, G. F.; Willis, A. C.; Wild, S. B. *Inorg. Chem.* **1997**, *36*, 1588–1597. (b) Cook, V. C.; Willis, A. C.; Zank, J.; Wild, S. B. *Inorg. Chem.* **2002**, *41*, 1897–1906. (c) Bowyer, P. K.; Cook, V. C.; Gharib-Naseri, N.; Gugger, P. A.; Rae, A. D.; Swiegers, G. F.; Willis, A. C.; Zank, J.; Wild, S. B. *Proc. Natl. Acad. Sci. U.S.A.* **2002**, *99*, 4877–4882.

- (10) Lützen, A.; Hapke, M.; Griep-Raming, J.; Haase, D.; Saak, W. *Angew. Chem., Int. Ed.* **2002**, *41*, 2086–2089.
- (11) Schalley, C. A.; Lützen, A.; Albrecht, M. *Chem.—Eur. J.* **2004**, *10*, 1072–1080.
- (12) (a) Kiehne, U.; Weilandt, T.; Lützen, A. *Org. Lett.* **2007**, *9*, 1283–1286. (b) Kiehne, U.; Weilandt, T.; Lützen, A. *Eur. J. Org. Chem.* **2008**, 2056–2064.
- (13) Kiehne, U.; Lützen, A. *Org. Lett.* **2007**, *9*, 5333–5336.
- (14) Tietze, L. F.; Eicher, T. In *Reaktionen und Synthesen im organisch-chemischen Praktikum und Forschungslaboratorium*, 2nd ed.; Thieme: Stuttgart, 1991; p 446.
- (15) Hu, Q.-S.; Vitharana, D.; Pu, L. *Tetrahedron: Asymmetry* **1995**, *6*, 2123–2126.
- (16) Cui, Y.; Evans, O. R.; Ngo, H. L.; White, P. S.; Lin, W. *Angew. Chem., Int. Ed.* **2002**, *41*, 1159–1162.
- (17) Ishitani, H.; Ueno, M.; Kobayashi, S. *J. Am. Chem. Soc.* **2000**, *122*, 8180–8186.
- (18) (a) Hama, Y.; Nobuhara, Y.; Aso, Y.; Otsubo, T.; Ogura, F. *Bull. Chem. Soc. Jpn.* **1988**, *61*, 1683–1686. (b) Dolci, L.; Dolle, F.; Valette, H.; Vaufray, F.; Fuseau, C.; Bottlaender, M.; Crouzel, C. *Bioorg. Med. Chem.* **1999**, *7*, 467–479.
- (19) Magidson, O.; Menchikov, G. *Ber.* **1925**, *58B*, 113–118.
- (20) Baxter, P. N. W. *J. Org. Chem.* **2000**, *65*, 1257–1272.
- (21) Daab, J. C.; Bracher, F. *Monatsh. Chem.* **2003**, *134*, 573–583.

Scheme 3. Synthesis of Pyridines **13** and **15**Scheme 4. Synthesis of the Bromopyridine **17**

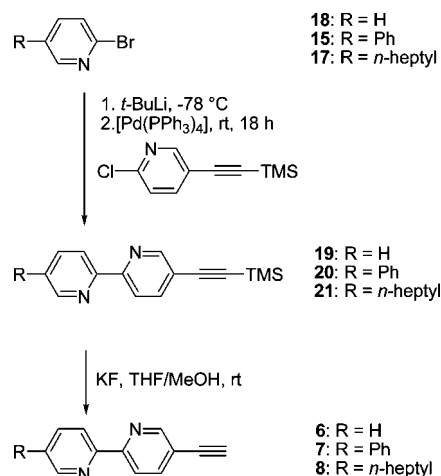
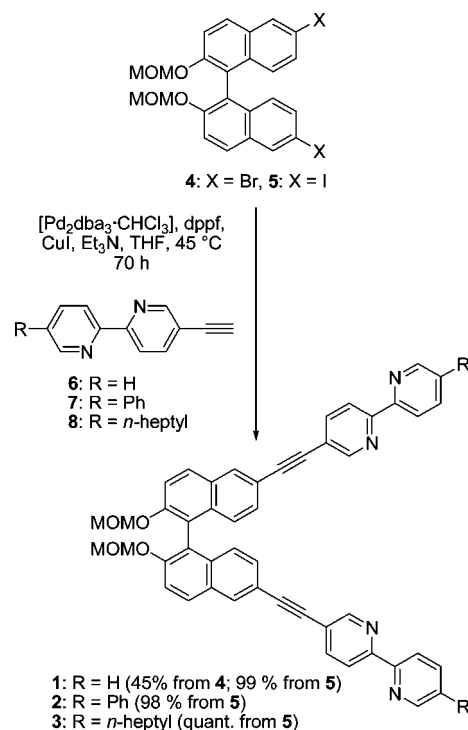
Sandmeyer reaction of **14** provided the respective bromide **15** in 88% yield (Scheme 3).²²

3-Picoline was first lithiated in benzylic position using LDA and then reacted with *n*-hexyl iodide to give **16**.²³ After 2-lithiation of **16** by treatment with LiDMEA and *n*-BuLi it was converted into 2-bromo-5-*n*-heptylpyridine (**17**) upon quenching with bromine (Scheme 4).²³

Bromopyridines **15** and **17** as well as commercially available 2-bromopyridine (**18**) were then transformed into the corresponding zinc organic compounds and subjected to our [Pd-(PPh₃)₄]-catalyzed modified Negishi cross-coupling reaction to give the TMS-ethynyl-functionalized 2,2'-bipyridines **19–21**.²³ Fluoride-promoted cleavage of the silyl protecting group finally afforded the desired 2,2'-bipyridines **6–8** (Scheme 5).

Target compounds (*M*)- and (*P*)-**1**, **2**, and **3** were finally obtained by 2-fold Sonogashira coupling of the dihalogenated BINOLs (*M*)- or (*P*)-**4** and (*M*)- or (*P*)-**5** with **6**, **7**, and **8**, respectively. It should be noted that excellent yields were obtained when [Pd₂dba₃·CHCl₃] and dppf were used together with the diiodide **5** instead of the less reactive dibromide **4**, although prolonged reactions times of 70 h were necessary (Scheme 6).

As hoped, the solubility of **3** proved to be much higher than the one of **1** in most organic solvents. The only exception was DMF, however, in which **1** was the best-soluble of the new

Scheme 5. Synthesis of 5-Ethynylated 2,2'-Bipyridines **6–8**Scheme 6. Synthesis of BINOL-Based Bis(bipyridines) (*M*)- and (*P*)-**1–3**

ligands. Unfortunately, the introduction of the phenyl groups in **2** did not have the desired effect to increase the solubility in aromatic solvents. By contrast, it even turned out to be the least soluble ligand of this family.

Metal Coordination. With the ligands in hands we started to study their coordination properties to diamagnetic late transition metal ions such as silver(I), copper(I), iron(II), and zinc(II). The first two usually prefer a 4-fold coordination in a tetrahedral geometry by two 2,2'-bipyridines, which should lead to dinuclear double-stranded helicates, whereas iron(II) ions form complexes with three bipyridines in an octahedral coordination geometry, eventually giving dinuclear triple-stranded helicates. Zinc(II), however, is a special case because it was found to form both 6-fold and 4-fold coordinated complexes, a behavior that has been described as a "chameleon" character.²⁴ Thus, the use of zinc cations can result in the formation of both species, which had already been observed by us earlier, by the exclusive

(22) Bouillon, A.; Lancelot, J.-C.; Collot, V.; Bovy, P. R.; Rault, S. *Tetrahedron* **2002**, *58*, 2885–2890.

(23) Kiehne, U.; Bunzen, J.; Staats, H.; Lützen, A. *Synthesis* **2007**, 1061–1069.

formation of triple-stranded helicates when using a 3,3'-difunctionalized BINOL-based bis(bipyridine) ligand on the one hand,¹⁰ but also an exclusive formation of double-stranded helicates in the case of a D-isomannide-based ligand on the other.¹³

Mixing solutions of the metal salts and the ligands in a 1:1 (metal:ligand) stoichiometry in the case of silver(I) and copper(I) and 2:3 for iron(II) and zinc(II) led to the expected color changes, indicating the successful formation of metal complexes: solutions of silver complexes had a slightly yellow tinge, the copper complexes had a brown-red color, the zinc complexes gave an intensive yellow color, and the iron complexes were deep red.

These solutions were then subjected to ESI-MS (Figures 1 and 2). The experiments proved the exclusive formation of discrete metallo-supramolecular species because only signals of intact dinuclear coordination compounds and fragments resulting from them could be detected, without any hints at oligo- or polymeric structures. These experiments gave the same trends for all three ligands **1–3**, indicating that the substitution with hydrocarbon groups in the 5'-position of the bipyridine does not interfere with the complex formation. In the following, we will thus focus on the complexes of **1** throughout the discussion.

The spectrum of the silver complex showed a signal at 839.1 m/z for the doubly charged $[\text{Ag}_2\mathbf{1}_2]^{2+}$ complex, which was mixed with its singly charged $[\text{Ag}\mathbf{1}]^+$ fragment complex (Figure 1a). The only other significant peak at 731.2 m/z resulted from the protonated ligand. This also seemed to be a fragment of the dinuclear complex, whose intensity (as well as the one of the $[\text{Ag}\mathbf{1}]^+$ fragment) could be modified to some extent by varying the experimental parameters, indicating that the silver(I) helicates are not totally stable under the condition of the ESI-MS experiments. The assumption that $[\text{Ag}\mathbf{1}]^+$ and $[\mathbf{1} + \text{H}]^+$ were really fragments and not species present in solution was corroborated by analysis of the NMR spectra, which showed no indications of any free ligand or a nonsymmetrical mononuclear complex, as will be discussed later. In addition, this behavior was in agreement with our previous findings with similar bis(bipyridine) ligands.

The spectrum of the copper complex (Figure 1b) showed only one dominant signal at 794.1 m/z , which undoubtedly belonged to the doubly charged $[\text{Cu}_2\mathbf{1}_2]^{2+}$ complex. This again is typical of these complexes and proved that they were more stable than the respective silver(I) analogues under the same ESI-MS experiment conditions. A similar behavior was observed for iron(II) complexes (Figure 1c). Here, the base peak at 575.9 m/z was attributed to the expected 4-fold charged 3:2 complex $[\text{Fe}_2\mathbf{1}_3]^{4+}$, which showed that iron indeed forms triple-stranded complexes with this ligand. Besides this the only other signal at 774.2 m/z could be assigned to an only partially dissociated 3:2 iron complex that still carries one fluoride counterion (originating from a decay of a tetrafluoroborate ion).

In the case of zinc(II), however, the situation was more complicated because we did not only find signals arising from the expected triple-stranded aggregate $[\text{Zn}_2\mathbf{1}_3]^{4+}$ (Figure 2) but also from a double-stranded complex $[\text{Zn}_2\mathbf{1}_2]^{4+}$ (the latter one mixed with the $[\text{Zn}\mathbf{1}]^{2+}$ fragment). Obviously, the helicate formation is not selective with respect to the stoichiometry of the resulting supramolecular assembly. This is interesting because a relatively small change in the ligand structure from

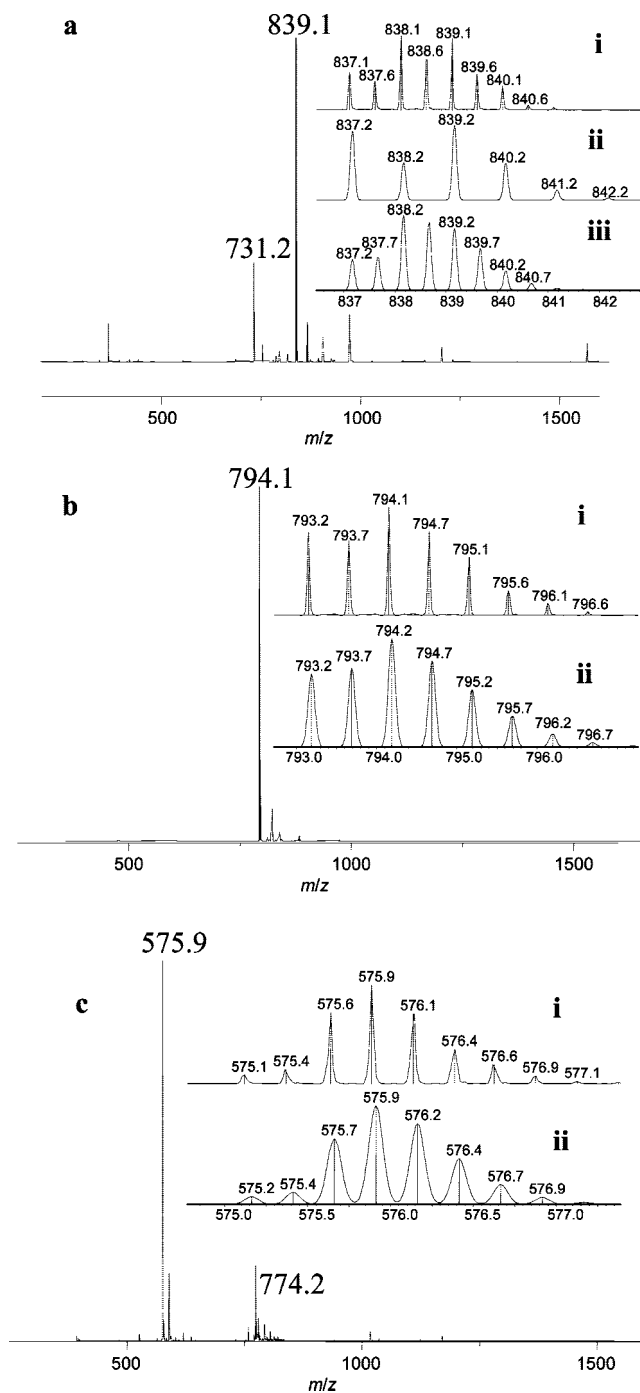


Figure 1. Positive ESI mass spectra of (a) the silver complex solution; inset (i) showing the mixed signal of $\{\text{Ag}_2(M)\mathbf{1}_2\}^{2+}$ and $\{\text{Ag}(M)\mathbf{1}\}^+$ at 839.1 m/z ; (ii) the calculated signal of $\{\text{Ag}_2(M)\mathbf{1}_2\}^{2+}$; and (iii) the calculated signal of $\{\text{Ag}(M)\mathbf{1}\}^+$; (b) the copper complex solution: (i) showing the signal of $\{\text{Cu}_2(M)\mathbf{1}_2\}^{2+}$; (ii) the calculated signal of $\{\text{Cu}_2(M)\mathbf{1}_2\}^{2+}$; (c) the iron complex solution (i) showing the signal of $\{\text{Fe}_2(M)\mathbf{1}_3\}^{4+}$ at 575.9 m/z ; (ii) the calculated signal of $\{\text{Fe}_2(M)\mathbf{1}_3\}^{4+}$ ($\text{CH}_2\text{Cl}_2/\text{CH}_3\text{CN}$ 1:1, 5×10^{-5} M).

a 3,3'-disubstituted BINOL core to a 6,6'-BINOL portion has a dramatic effect on the ability of the ligand to form complexes with zinc(II): While our new ligands **1–3** with a 6,6'-disubstituted BINOL were found to lack almost any preference for the formation of double- or triple stranded helicates, our older one, based on a 3,3'-disubstituted BINOL, was found to undergo both stoichiometrically selective and diastereoselective self-assembly upon coordination to zinc(II) ions.

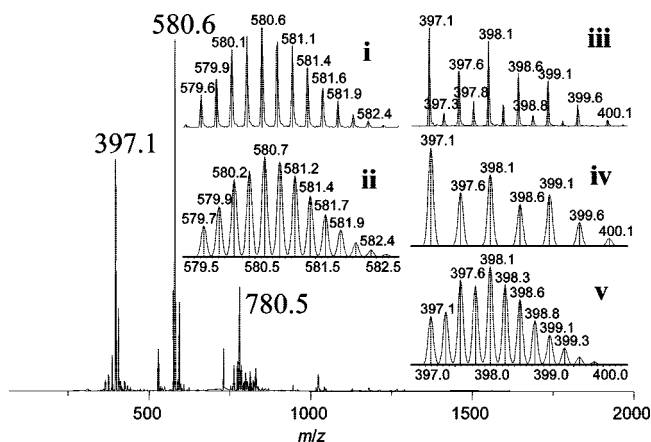


Figure 2. Positive ESI mass spectrum of the zinc complex solution (i) showing the magnified signal of $\{Zn_2[(M)-1]_3\}^{2+}$ at 580.6 m/z ; (ii) the calculated signal of $\{Zn_2[(M)-1]_3\}^{4+}$; (iii) showing the mixed magnified signal of $\{Zn_2[(M)-1]_2\}^{4+}$ and $\{Zn(M)-1\}^{2+}$ at 397.1 m/z ; (iv) the calculated signal for $\{Zn(M)-1\}^{2+}$; (v) the signal calculated for $\{Zn_2[(M)-1]_2\}^{4+}$ (CH_2Cl_2/CH_3CN 1:1, 5×10^{-5} M).

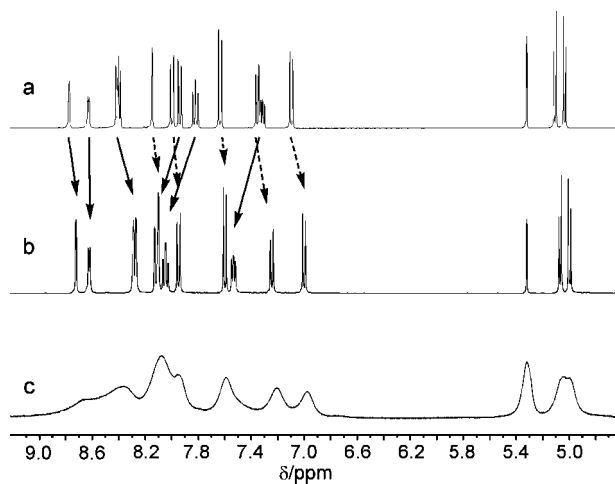


Figure 3. 1H NMR spectra of ligand (*M*)-1 in $DMF-d_7$ at 298 K (a) free ligand; (b) 1:1 complex of (*M*)-1 with $[Ag(CH_3CN)_4BF_4]$; (c) 1:1 complex of (*M*)-1 with $[Cu(CH_3CN)_4BF_4]$ (CD_2Cl_2/CD_3CN 5:2, 3 mmol L^{-1}).

Further insight into the (stereo)selectivity of the self-assembly processes was expected from NMR spectroscopy. The silver(I) complexes of **1–3** gave rise to very sharp and distinct NMR signals (Figure 3b).

From the analysis of these spectra, several conclusions could be drawn, as discussed exemplarily for $[Ag_2I_2](BF_4)_2$. First, the signals of the complex were considerably shifted compared to those of the free ligand. The shifts of the bipyridine proton signals (black arrows) were easily explained by the complexation to the silver ion, whereas the upfield shift of the BINOL-derived proton signals (dashed arrows) resulted from the change of the angle between the naphthyl rings of the BINOL, both indications for a successful and complete formation of a silver complex. Second, the spectrum of the silver(I) complex showed the same number of signals as the one of the free ligand. Thus, the symmetry of the enantiomerically pure ligand must have been retained in the metallo-supramolecular assembly. Hence, the formation of mononuclear complexes could be ruled out, because the spectra should be more complicated.

Figure 4 shows the three possible diastereomeric double-stranded helicates that can in principle be formed from enantiopure (*M*)-1 (MOM groups are omitted for viewing clarity).

From these the “meso”-like diastereomer,²⁵ with oppositely configured metal centers (and hence diastereomorphous portions) could also be ruled out for the same reason as the mononuclear complex. Thus, the only two assemblies remaining were dinuclear helicates with either (Δ,Δ)- or (Λ,Λ)-configured (chirality descriptors according to the *oriented line* system)^{26,27} metal centers, i.e., with homomorphous portions. These, however, are diastereomers, and it is rather unlikely that all of their proton signals should be isochronic by coincidence. Thus, the self-assembly process is indeed highly diastereoselective, leading to stereochemically pure helicates.

Unfortunately, the spectra of the zinc, copper, and iron complexes recorded in either a mixture of CD_2Cl_2/CD_3CN or just in $DMF-d_7$ at room temperature showed only very broad signals (see Figure 3c). Temperature dependent measurements in these solvents did not help to get better spectra by slowing down this process because the complexes tend to precipitate from solutions around 0 °C. As observed^{10–13} and proven¹⁰ in previous studies by ESI-MS experiments with isotopically labeled ligands, this is a result of fast ligand-exchange processes rather than a consequence of oligomer formation (although intramolecular rearrangement processes could not be ruled out completely either). This was further confirmed by dilution experiments because the spectra did not change even at concentrations similar to those used for the MS experiments, which ruled out the presence of oligomeric species at a concentration of 5×10^{-5} mol L^{-1} . In the case of iron the dynamic processes could be slowed down considerably by changing the solvent to a 3:1 mixture of dichloromethane- d_2 and $DMSO-d_6$ (Figure 5). Under these conditions, again sharp signals were obtained that also prove that the iron salt is not contaminated by paramagnetic iron(III) ions, which could have been another reason for the signal broadening. The stoichiometry of the complexes was again confirmed by ESI-MS. After one day, the reaction mixture had converged to mainly one clearly dominant complex. In fact, the dynamics to reach this final preference is so slow that one can detect several species after 1 h of mixing. The diastereoselectivity, however, is not as perfect as in the case of the double-stranded silver helicates although it is still very high. For the same reasons given for the silver helicate the dominant iron helicate is also *D*-symmetric, consisting of two homomorphous portions.

Although we did not get single crystals suitable for an X-ray analysis to assign the stereochemistry of the metal centers, we succeeded in establishing the relative and thus, given the known axial configuration of the BINOL portion, the absolute orientation of the 2,2'-bipyridine unit and the BINOL core by using ROESY-NMR spectroscopy and CD experiments together with quantum chemical calculations. According to DFT calculations, the aromatic systems of bipyridine and BINOL should be nearly coplanar in the (Λ,Λ)-complex, which should result in marked ROE contacts between H-7 and H-17 and between H-5 and the protons at C-14, like it had been found in previous cases.¹⁰ But instead, ROE contacts between H-5 with H-14 and H-17 as well as ROEs between H-7 with H-14 and H-17 were observed (Figure 6). This indicated that the two aromatic systems are

(25) Please note this is not a real meso-compound. In fact this aggregate would be even less symmetrical than the helicates with (*D,D*)- or (*L,L*)-configured metal centers because of the stereogenic axes in the ligand structure (C_2 vs D_2 or C_3 vs D_3).

(26) Damhus, T.; Schaeffer, C. E. *Inorg. Chem.* **1983**, *22*, 2406–2412.

(27) Zelewsky, A. v. *Stereochemistry of Coordination Compounds*; John Wiley & Sons: Chichester, 1996. For a concise description of the use of the oriented-line and the skew-line system see also ref 13.

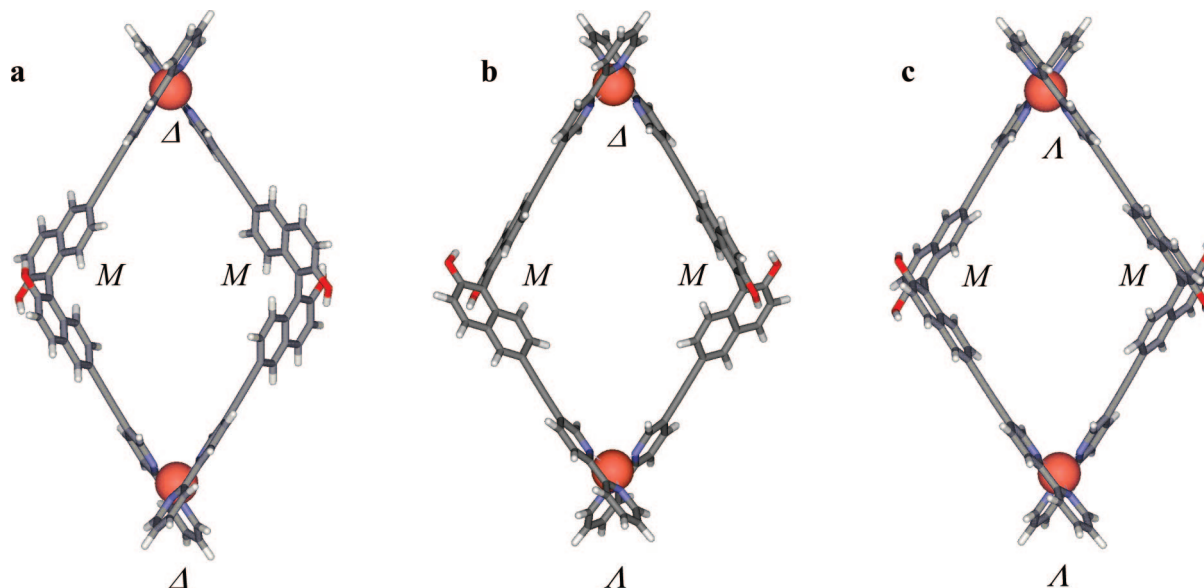


Figure 4. RI-BLYP/SVP (TZVP for copper) optimized complexes of (*M*)-**1** with Cu⁺ (a) (Δ,Δ) complex; (b) (Δ,Λ)-complex; (c) (Λ,Λ)-complex.

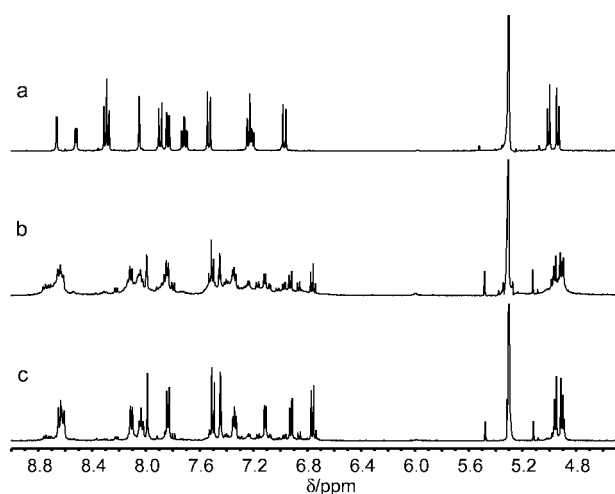


Figure 5. ¹H NMR spectra of ligand (*M*)-**1** in CD₂Cl₂/DMSO-*d*₆ 3:1 at 298 K (a) free ligand (400 MHz, 1 mmol L⁻¹); (b) 3:2 mixture of (*M*)-**1** with Fe(BF₄)₂·6H₂O 30 min after mixing (500 MHz, 1 mmol L⁻¹); (c) 3:2 mixture of (*M*)-**1** with Fe(BF₄)₂·6H₂O 24 h after mixing (500 MHz, 1 mmol L⁻¹).

twisted, which seems more pronounced in the (Δ,Δ)-stereoisomer. This assignment was initially rather surprising for us because the 3,3'-substituted BINOL ligands with (*M*)-configuration selectively form (Λ,Λ)-configured complexes whereas the 6,6'-substituted ligand (*M*)-**1** seems to induce the exclusive formation of (Δ,Δ)-configured assemblies.

Because the observed ROEs are in general small and ROESY spectra are sometimes prone to TOCSY and/or COSY artifacts,²⁸ the use of another, independent method seemed necessary to prove this assignment, which would also allow the analysis of the copper(I) and iron(II) helicates. To study our complexes in solution, chiroptical methods appeared to be ideal.^{27,29} The CD spectra obtained for the two silver helicates of (*M*)- and (*P*)-**1** (see Figure 7a) showed that these two complexes were indeed

enantiomers as expected from their identical NMR spectra. In Figure 7b the CD spectrum of the silver helicate of (*M*)-**1** is compared with those recorded from the ligand (*M*)-**1** itself and its copper(I) and the iron(II) helicates.

The analysis of these spectra led to the conclusion that the copper(I) and the silver(I) helicates as well as the major iron(II) helicate that dominates the spectrum should have the same configuration because of the quite similar CD curves. All complexes and the free ligand did show a rather dominant Cotton effect in the 230 to 275 nm region, which is caused by the chiral biaryl axis. The exciton chirality method confirmed the (*M*)-configuration of this axis because of a first (i.e., long-wavelength) negative Cotton effect, followed by a second, positive one. More important for the intact complexes is the first Cotton effect at 375 nm for the silver(I) and copper(I) complexes, and at 400 nm for the iron(II) complex, which is negative for all complexes possessing (*M*)-configured axes. Thus, compared to related structures from the literature,^{13,26,29,30} the (*M*)-configured ligand gives rise to (Δ,Δ)-configured helices therefore indicating a *P*-helix (according to the oriented-line system, see above),^{26,27} which is in accordance with our ROESY-NMR results.

For a further confirmation of this stereochemical assignment, the CD-spectra of the complex solutions were calculated. Therefore, the structures of the (Δ,Δ)- and the (Λ,Λ)-configured dinuclear silver(I) and iron(II) helicates were optimized with RI-BLYP³¹ using the TZVP³² basis set for the metal atoms and the SVP³³ basis set for the other atoms. ZINDO/S-CIS calculations of the found global minima of the complexes resulted in CD spectra that were then compared with the experimental ones. As Figure 8 shows, the spectra calculated for the (Δ,Δ)-configured complexes fit much better with the experimental ones

(28) Claridge, T. D. W. *High-Resolution NMR Techniques in Organic Chemistry*; Pergamon: Amsterdam, 1999.

(29) Ziegler, M.; von Zelewsky, A. *Coord. Chem. Rev.* **1998**, *177*, 257–300.

(30) (a) Mamula, O.; von Zelewsky, A.; Bernardinelli, G. *Angew. Chem., Int. Ed.* **1998**, *37*, 290–293. (b) Telfer, S. G.; Kuroda, R.; Sato, T. *Chem. Commun.* **2003**, 1064–1065. See also ref 7d.

(31) (a) Becke, A. D. *Phys. Rev. A* **1988**, *38*, 3098–3100. (b) Lee, C.; Yang, W.; Parr, R. G. *Phys. Rev. B* **1988**, *37*, 785–789.

(32) Schäfer, A.; Huber, C.; Ahlrichs, R. *J. Chem. Phys.* **1994**, *100*, 5829–5835.

(33) Schäfer, A.; Horn, H.; Ahlrichs, R. *J. Chem. Phys.* **1992**, *97*, 2571–2577.

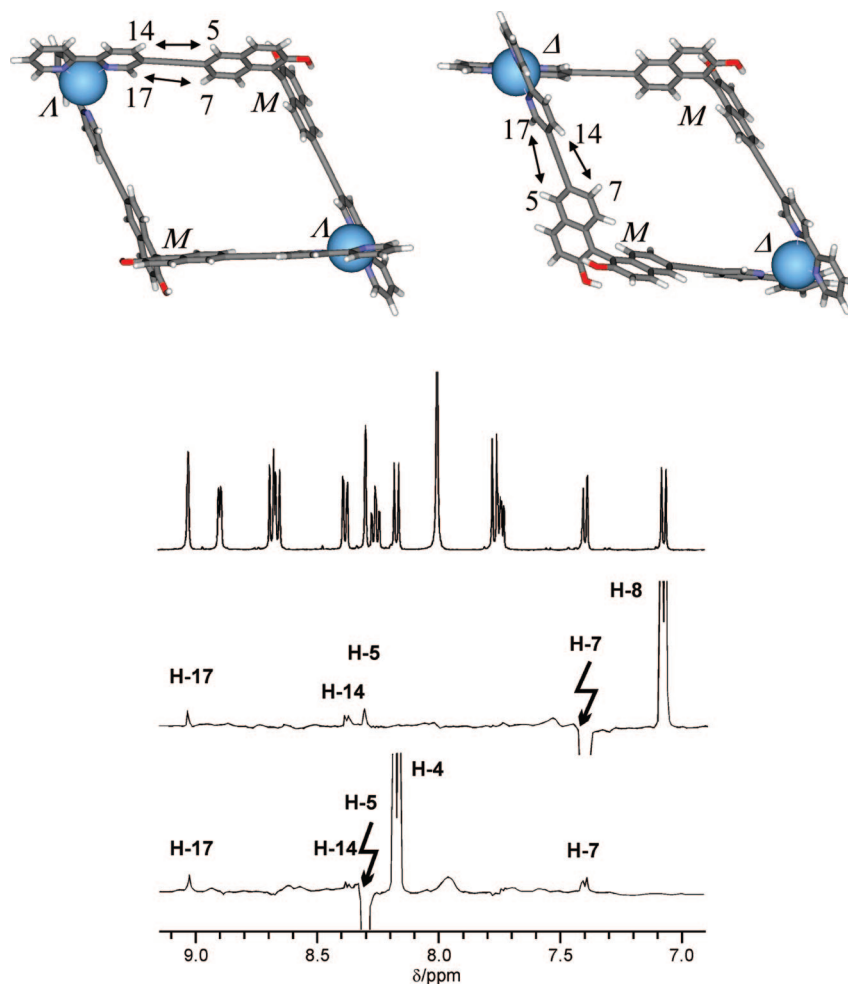


Figure 6. RI-BLYP/SVP (TZVP for the Ag atoms) minimized 2:2 complexes of (*M*)-**1** with Ag⁺, (Δ,Δ) (left), (Λ,Λ) (right), and extension of two relevant 1D traces of the gs-2D-ROESY-NMR spectrum in DMF-*d*₇ at 298 K.

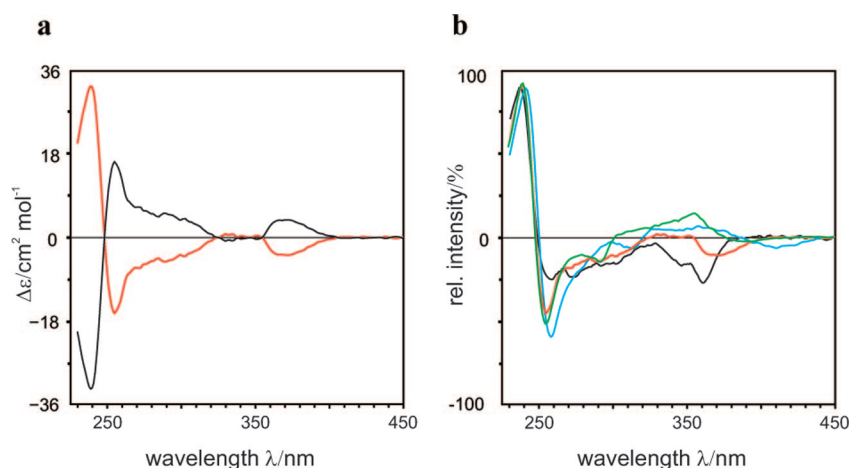


Figure 7. CD spectra measured in CH₂Cl₂/CH₃CN 9:1, 5×10^{-5} mol L⁻¹ at room temperature: (a) spectra of {Ag₂[(*M*)-**1**]₂}(BF₄)₂ (black) and {Ag₂[(*P*)-**1**]₂}(BF₄)₂ (red); (b) spectra of (*M*)-**1** (black), {Ag₂[(*M*)-**1**]₂}(BF₄)₂ (red), {Cu₂[(*M*)-**1**]₂}(BF₄)₂ (green), and {Fe₂[(*M*)-**1**]₃}(BF₄)₄ (blue).

(in the case of iron, one has to take into account that there is also at least one additional, minor species present, whose stereostructure, however, could not be elucidated) than those computed for (Λ,Λ), unambiguously demonstrating that the complex diastereoselectively formed when using the (*M*)-ligand was (Δ,Δ)-configured, and, consequently, the one formed with the (*P*)-ligand was (Λ,Λ).

Conclusion

We have succeeded in synthesizing three members of a new class of bis(bipyridine) ligands based on a 6,6'-disubstituted BINOL core in 11 (for **1**) and 13 steps (for **2** and **3**). These ligands were demonstrated to form dinuclear coordination compounds with late transition metal ions such as copper(I), silver(I), iron(II), and zinc(II). The zinc(II) complexes were

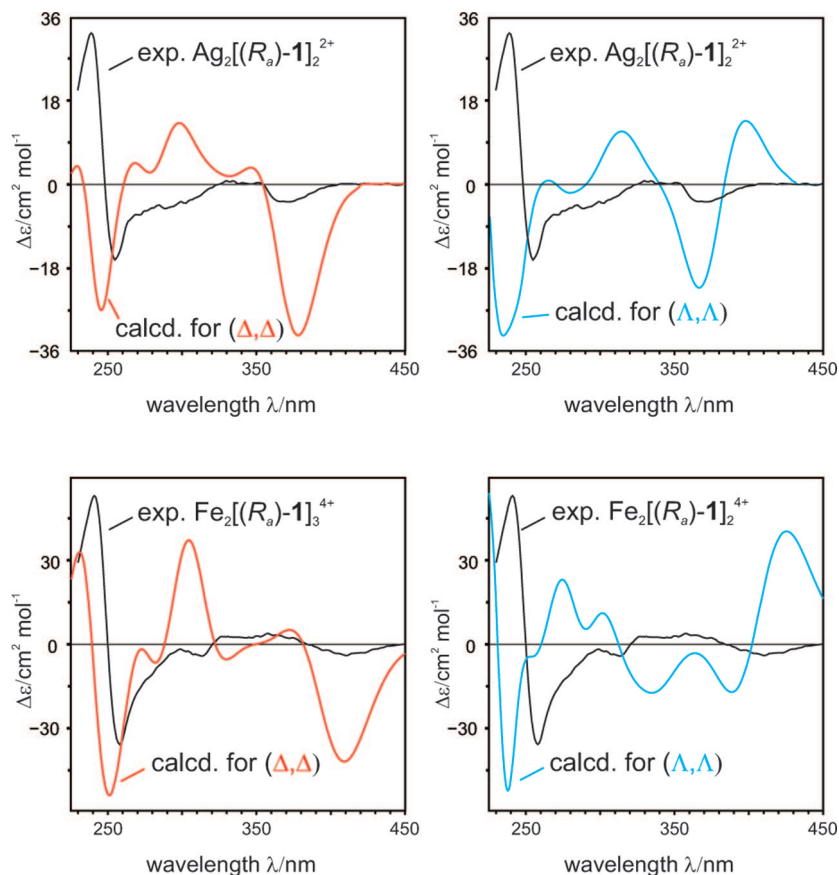


Figure 8. CD spectra of the silver (top) and iron complexes (bottom), experimental (black lines) and calculated for the (Δ,Δ) - (red lines, left) and for the (Λ,Λ) -configured (blue lines, right) complexes formed with (M) -configured ligand **1** in $\text{CH}_2\text{Cl}_2/\text{CH}_3\text{CN}$ 9:1, $5 \times 10^{-5} \text{ mol L}^{-1}$ at room temperature.

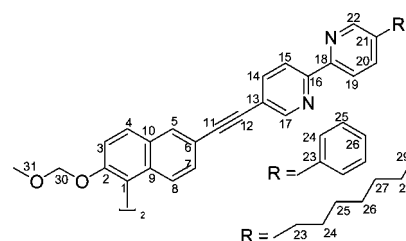
found to be a complex mixture of different double- and triple-stranded aggregates. In the case of copper, silver, and iron, however, the ligands underwent completely diastereoselective self-assembly to enantiomerically pure double- (copper and silver) and highly diastereomeric self-assembly to triple-stranded helicates (iron). For the silver helicates, ROESY-NMR spectroscopy was successfully applied to assign the configuration at the newly formed stereogenic metal centers. This assignment was further corroborated by CD spectroscopy in combination with theoretical calculations. These studies clearly prove that the (M) -enantiomers of the ligands preferably induce a (Δ,Δ) -configuration of the metallo-supramolecular assemblies, whereas the (P) -configured ligands lead to the formation of the enantiomeric (Λ,Λ) -complexes thus giving rise to chiral cavities in a simple and highly stereocontrolled manner. We are currently broadening the scope of BINOL-based helical metal complexes by exploring further elaborated ligand designs.

Experimental Section

All solvents were distilled and thoroughly dried prior to use according to standard procedures. All syntheses with air- and moisture-sensitive compounds were performed under Schlenk conditions, with argon as the inert gas. For purification purposes, column chromatography on silica gel and preparative thin layer chromatography with silica gel layers was applied. Solvents for mobile phases were distilled prior to use. Detection was done under UV light (254 and 366 nm).

^1H and ^{13}C NMR spectra were recorded at 298 K, at 500.1 and 125.8 MHz, or at 298 K, at 400.1 and 100.6 MHz, respectively. ^1H NMR chemical shifts are reported on the δ scale (ppm) relative to residual nondeuterated solvent as the internal standard. ^{13}C NMR

Scheme 7. Numbering of Atoms for NMR Assignment



chemical shifts are given in δ values (ppm) relative to the deuterated solvent as the internal standard. Signals were assigned on the basis of ^1H , ^{13}C , HMQC, HMBC, and ROESY NMR experiments. Numbering of the ^1H and ^{13}C nuclei is according to Scheme 7. Melting points are not corrected. Chemicals and reagents (except for the solvents) obtained from commercial sources were used as received. The following compounds were prepared according to published procedures: (M) - and (P) -2,2'-dihydroxy-1,1'-binaphthyl [(M)- and (P) -**9**],^{14,15} (M) - and (P) -6,6'-dibromo-2,2'-dihydroxy-1,1'-binaphthyl [(M)- and (P) -**10**],¹⁶ (M) - and (P) -6,6'-dibromo-2,2'-dimethoxymethoxy-1,1'-binaphthyl [(M)- and (P) -**4**],¹⁷ (M) - and (P) -6,6'-diiodo-2,2'-dimethoxymethoxy-1,1'-binaphthyl [(M)- and (P) -**5**],¹⁷ 2-amino-5-iodopyridine (**11**),¹⁸ 2-chloro-5-iodopyridine (**12**),¹⁹ 2-chloro-5-[(trimethylsilyl)ethynyl]pyridine (**13**),²⁰ 2-amino-5-phenylpyridine (**14**),²¹ 2-bromo-5-phenylpyridine (**15**),²² 3-*n*-heptylpyridine (**16**),²³ 2-bromo-5-*n*-heptylpyridine (**17**),²³ 5-[(trimethylsilyl)ethynyl]-2,2'-bipyridine (**19**),²³ 5-phenyl-5'-[(trimethylsilyl)ethynyl]-2,2'-bipyridine (**20**),²³ 5-*n*-heptyl-5'-[(trimethylsilyl)ethynyl]-2,2'-bipyridine (**21**),²³ 5-ethynyl-2,2'-bipyridine (**6**),²³ 5-ethynyl-5'-phenyl-2,2'-bipyridine (**7**),²³ 5-ethynyl-5'-*n*-heptyl-2,2'-bipyridine (**8**).²³

Computational Details. All complexes were optimized with RI-BLYP³¹ and the basis set for all metal atoms was TZVP³² while SVP³³ was used for all other atoms. Starting from the found global minimum structures, ZINDO/S-CI³⁴ calculations yielded excitations (120 for the silver and copper complexes, 225 for the iron complexes) with the corresponding oscillator and rotational strength values (length formalism). The UV and CD curves were calculated as sums of Gaussian functions centered at the wavelength of the corresponding excitations and multiplied by the respective oscillator and rotational strength values. For both CD and UV spectra, an empirically chosen exponential half-width of 0.08 eV was used. Before comparison with the experimental CD spectra, all calculated ones were UV corrected (silver complexes –23 nm, iron complexes –28 nm).³⁵ All optimizations and the excited states calculations were done using the ab initio software package ORCA³⁶ while the subsequent Gauss-curve generation and the UV corrections were performed with SpecDis.³⁷

Synthesis of Ligands 1–3. A mixture of 101 mg (0.19 mmol, 1 equiv) of (*M*)- or (*P*)-2,2'-bis(methoxymethoxy)-6,6'-dibromo-1,1'-binaphthyl (**4**) or 119 mg (0.19 mmol, 1 equiv) of (*M*)- or (*P*)-2,2'-bis(methoxymethoxy)-6,6'-diiodo-1,1'-binaphthyl (**5**), 70 mg (0.39 mmol, 2.1 equiv) of 5-ethynyl-2,2'-bipyridine (**6**), 100 mg (0.39 mmol, 2.1 equiv) of 5-ethynyl-5'-phenyl-2,2'-bipyridine (**7**), or 111 mg (0.39 mmol, 2.1 equiv) of 5-ethynyl-5'-*n*-heptyl-2,2'-bipyridine (**8**), 8 mg (7.6 μmol, 4 mol-%) of Pd₂dba₃·CHCl₃, 8.5 mg (15.2 μmol, 8 mol-%) of 1,1'-diphenylphosphinoferrocene (dppf), and 6 mg (30.4 μmol, 16 mol-%) of CuI was thoroughly evacuated and flushed with argon. Ten milliliters of dry triethylamine and 4 mL of dry tetrahydrofuran were added, and the reaction solution was heated to 45 °C and stirred at this temperature for 70 h. After the mixture was cooled to rt, saturated ethylenediaminetetraacetic acid (EDTA) and sodium carbonate solutions in water were added, and the mixture was stirred for 15 min. The aqueous solution was extracted with dichloromethane. The organic layer was dried with sodium sulfate. After evaporation of the solvents, the remaining solid was purified by flash column chromatography using silica gel and the solvent system indicated for the respective compound.

(*M*)- or (*P*)-2,2'-Bis(methoxymethoxy)-6,6'-bis(5-ethynyl-2,2'-bipyridyl)-1,1'-binaphthyl (1**).** Column chromatography was performed using *n*-hexane/ethyl acetate/triethylamine 1:1:0.05 as the eluent; *R*_f = 0.5; yield: 62 mg (45%) starting from **4**; 137 mg (99%) starting from **5**; white solid; mp ≥ 225 °C; ¹H NMR (400 MHz, CDCl₃) δ 3.18 (s, 6 H, H-31), 5.02 (d, 2 H, H-30, ²*J*_{30,30'} = –6.9 Hz), 5.14 (d, 2 H, H-30', ²*J*_{30',30} = –6.9 Hz), 7.16 (d, 2 H, H-8, ³*J*_{8,7} = 8.8 Hz), 7.31 (ddd, 2 H, H-21, ³*J*_{21,22} = 7.8 Hz, ³*J*_{21,20} = 7.4 Hz, ⁴*J*_{21,19} = 1.8 Hz), 7.37 (dd, 2 H, H-7, ³*J*_{7,8} = 8.7 Hz, ⁴*J*_{7,5} = 1.5 Hz), 7.63 (d, 2 H, H-3, ³*J*_{3,4} = 9.1 Hz), 7.82 (ddd, 2 H, H-20, ³*J*_{20,21} = 7.4 Hz, ³*J*_{20,19} = 7.8 Hz, ⁴*J*_{20,22} = 1.4 Hz), 7.93–7.99 (m, 4 H, H-4, H-14), 8.15 (d, 2 H, H-5, ⁴*J*_{5,7} = 1.5 Hz), 8.40–8.43 (m, 4 H, H-15, H-19), 8.69 (ddd, 2 H, H-22, ³*J*_{22,21} = 7.8 Hz, ⁴*J*_{22,20} = 1.4 Hz, ⁵*J*_{22,19} = 0.8 Hz), 8.83 (dd, 2 H, H-17, ⁴*J*_{17,14} = 2.1 Hz, ⁵*J*_{17,15} = 0.7 Hz) ppm; ¹³C NMR (100.6 MHz, CDCl₃) δ 56.1 (C-31), 86.6 (C-12), 94.2 (C-11), 95.0 (C-30), 117.7 (C-3), 118.2 (C-1), 120.5 (C-15), 120.6 (C-6)*, 120.8 (C-13)*, 121.5 (C-19), 124.0 (C-21), 125.8 (C-8), 128.9 (C-7), 129.5 (C-10), 129.8 (C-4), 132.1 (C-5), 133.8 (C-9), 137.1 (C-20), 139.5 (C-14), 149.4 (C-22), 151.8 (C-17), 153.8 (C-2), 154.9 (C-16), 155.6 (C-18) ppm (* signal assignments might be interchanged); MS (EI): *m/z* (%) = 730.2 (100) [C₄₈H₃₄N₄O₄]⁺; HRMS (EI): calcd for [C₄₈H₃₄N₄O₄]⁺ 730.258,

found 730.2598; RP: (*M*-**1**): = –254.1° (*c* = 0.62, CH₂Cl₂), (*P*-**1**): = +232.6° (*c* = 0.55, CH₂Cl₂); CD [λ (Δε)]: (*M*) = 237 (15.5), 258 (–4.2), 360 (–4.5); (*P*) = 236 (–14.4), 257 (4.0), 361 (3.8).

(*M*)- or (*P*)-2,2'-Bis(methoxymethoxy)-6,6'-bis(5-ethynyl-5'-phenyl-2,2'-bipyridyl)-1,1'-binaphthyl (2**).** Column chromatography was performed using *n*-hexane/ethyl acetate/triethylamine 1:1:1 as the eluent; *R*_f = 0.4; yield: 164 mg (98%); yellow solid; mp ≥ 225 °C; ¹H NMR (400 MHz, CDCl₃) δ 3.19 (s, 6 H, H-31), 5.03 (d, 2 H, H-30, ²*J*_{30,30'} = –6.9 Hz), 5.15 (d, 2 H, H-30', ²*J*_{30',30} = –6.9 Hz), 7.18 (d, 2 H, H-8, ³*J*_{8,7} = 8.7 Hz), 7.36–7.45 (m, 4 H, H-7, H-26), 7.50 (dd, 4 H, H-25, ³*J*_{25,24} = 7.5 Hz, ³*J*_{25,26} = 7.7 Hz), 7.61–7.64 (m, 6 H, H-3, H-24), 7.94–8.00 (m, 4 H, H-4, H-14), 8.02 (dd, 2 H, H-20, ³*J*_{20,19} = 8.2 Hz, ⁴*J*_{20,22} = 2.1 Hz), 8.16 (s, 2 H, H-5), 8.45 (d, 2 H, H-15, ³*J*_{15,14} = 8.4 Hz), 8.49 (d, 2 H, H-19, ³*J*_{19,20} = 8.2 Hz), 8.85 (s, 2 H, H-17), 8.93 (d, 2 H, H-22, ⁴*J*_{22,20} = 2.1 Hz) ppm; ¹³C NMR (100.6 MHz, CDCl₃) δ 56.1 (C-31), 86.7 (C-12), 94.3 (C-11), 95.0 (C-30), 117.7 (C-3), 118.2 (C-1), 120.4 (C-15), 120.5 (C-13), 120.8 (C-6), 121.4 (C-19), 125.8 (C-8), 127.2 (C-24), 128.4 (C-26), 128.9 (C-7), 129.3 (C-25), 129.4 (C-10), 129.8 (C-4), 132.1 (C-5), 133.8 (C-9), 135.3 (C-20), 136.8 (C-21), 137.6 (C-23), 139.4 (C-14), 147.9 (C-22), 151.8 (C-17), 153.8 (C-2), 154.4 (C-18), 154.6 (C-16) ppm; MS (ESI, pos): *m/z* (%) = 883.3 (100) [C₆₀H₄₂N₄O₄ + H]⁺; HRMS (ESI, pos): calcd for [C₆₀H₄₂N₄O₄ + H]⁺ 883.3279, found 883.3261; RP: (*M*-**2**): = –261.4° (*c* = 0.535, CH₂Cl₂), (*P*-**2**): = +279.0° (*c* = 0.365, CH₂Cl₂); CD [λ (Δε)]: (*M*) = 233 (18.5), 257 (–5.5), 369 (–6.4); (*P*) = 233 (–17.5), 258 (5.1), 370 (6.2).

(*M*)- or (*P*)-2,2'-Bis(methoxymethoxy)-6,6'-bis(5-ethynyl-5'-heptyl-2,2'-bipyridyl)-1,1'-binaphthyl (3**).** Column chromatography was performed using *n*-hexane/ethyl acetate + triethylamine 5:1 + 5% as the eluent; *R*_f = 0.25; yield: 176 mg (quant.); yellow solid; mp = 157 °C; ¹H NMR (400 MHz, CDCl₃) δ 0.88 (t, 6 H, H-29, ³*J*_{29,28} = 7.1 Hz), 1.22–1.39 (m, 16 H, H-25, H-26, H-27, H-28), 1.61–1.70 (m, 4 H, H-24), 2.66 (t, 4 H, H-23, ³*J*_{23,24} = 7.8 Hz), 3.18 (s, 6 H, H-31), 5.02 (d, 2 H, H-30, ²*J*_{30,30'} = –6.9 Hz), 5.14 (d, 2 H, H-30', ²*J*_{30',30} = –6.9 Hz), 7.16 (d, 2 H, H-8, ³*J*_{8,7} = 8.8 Hz), 7.37 (dd, 2 H, H-7, ³*J*_{7,8} = 8.7 Hz, ⁴*J*_{7,5} = 1.7 Hz), 7.61–7.66 (m, 4 H, H-3, H-20), 7.93 (dd, 2 H, H-14, ³*J*_{14,15} = 8.3 Hz, ⁴*J*_{14,17} = 2.2 Hz), 7.96 (d, 2 H, H-4, ³*J*_{4,3} = 9.0 Hz), 8.15 (d, 2 H, H-5, ⁴*J*_{5,7} = 1.7 Hz), 8.32 (d, 2 H, H-19, ³*J*_{19,20} = 8.1 Hz), 8.38 (dd, 2 H, H-15, ³*J*_{15,14} = 8.3 Hz, ⁵*J*_{15,17} = 0.8 Hz), 8.51 (d, 2 H, H-22, ⁴*J*_{22,20} = 1.8 Hz), 8.81 (d, 2 H, H-17, ⁴*J*_{17,14} = 2.2 Hz, ⁵*J*_{17,15} = 0.8 Hz) ppm; ¹³C NMR (100.6 MHz, CDCl₃) δ 14.2 (C-29), 22.8 (C-28), 29.21 (C-27)*, 29.22 (C-26)*, 31.2 (C-24), 31.9 (C-25), 33.0 (C-23), 56.1 (C-31), 86.7 (C-12), 94.0 (C-11), 95.0 (C-30), 117.7 (C-3), 118.2 (C-6), 120.17 (C-13), 120.18 (C-15), 120.8 (C-1), 121.1 (C-19), 125.8 (C-8), 128.9 (C-7), 129.5 (C-10), 129.8 (C-4), 132.1 (C-5), 133.8 (C-9), 136.9 (C-20), 138.7 (C-21), 139.4 (C-14), 149.6 (C-22), 151.7 (C-17), 153.3 (C-18), 153.7 (C-2), 155.1 (C-16) ppm (* signal assignment might be interchanged); MS (ESI, pos): *m/z* (%) = 927.5 (60) [C₆₂H₆₂N₄O₄ + H]⁺ 464.2 (100) [C₆₂H₆₂N₄O₄ + 2H]²⁺; EA: calcd for [C₆₂H₆₂N₄O₄ + 2/3CH₂Cl₂] C 76.51 H 6.49 N 5.69, found C 76.52 H 6.54 N 5.68; HRMS (ESI, pos): calcd for [C₆₂H₆₂N₄O₄ + H]⁺ 927.4844, found 927.4849; RP: (*M*-**3**): = –230.0° (*c* = 0.46 CH₂Cl₂), (*P*-**3**): = +213.4° (*c* = 0.63 CH₂Cl₂); CD [λ (Δε)]: (*M*) = 237 (15.0), 256 (–6.0), 363 (–6.1); (*P*) = 234 (–14.1), 258 (4.7), 362 (5.0).

Preparation of Metal Complexes Exemplified for the Synthesis of {Ag₂(*M*-1**)₂}(BF₄)₂.** A 6.00 mg (8.21 μmol) amount of (*M*-**1**) and 2.272 mg (8.21 μmol) of [Ag(CH₃CN)₂]BF₄ were dissolved in 0.5 mL of CD₂Cl₂ or DMF-*d*₇ (ligand) and 0.2 mL CD₃CN or DMF-*d*₇ (salt). The two solutions were combined and mixed. The resulting light yellow solution was transferred into an NMR tube. Likewise, solutions for measurement of ESI- and CD-spectra were generated. For ESI-MS studies a 1 × 10^{–4} mol L^{–1} solution was generated (CH₂Cl₂/CH₃CN 1:1) and for CD a 5 × 10^{–5} mol L^{–1} solution (CH₂Cl₂/CH₃CN 9:1).

{Ag₂(*M*-**1**)₂}(BF₄)₂/{Ag(*P*-**1**)}(BF₄). ¹H NMR (400 MHz, DMF-*d*₇) δ 3.18 (s, 12 H, H-31), 5.19 (d, 4 H, H-30, ²*J*_{30,30'} =

(34) Ridley, J.; Zerner, M. *Theor. Chim. Acta* **1973**, *32*, 111–134.

(35) Bringmann, G.; Busemann, S. In *Natural Product Analysis: Chromatography, Spectroscopy, Biological Testing*; Schreier, P., Herderich, M., Humpf, H.-U., Schwab, W., Eds.; Vieweg: Wiesbaden, 1998; pp 195–211.

(36) Neese, F. ORCA - An ab-initio, DFT and SCF-MO package, Version 2.6.35; Universität Bonn, Bonn, Germany, 2008.

(37) Bruhn, T.; Maksimenka, K.; Bringmann, G. SpecDis, Version 1.35; Universität Würzburg, Würzburg, Germany, 2008.

−6.8 Hz), 5.25 (d, 4 H, H-30', $^2J_{30',30} = -6.8$ Hz), 7.11 (d, 4 H, H-8, $^3J_{8,7} = 8.8$ Hz), 7.43 (dd, 4 H, H-7, $^3J_{7,8} = 8.8$ Hz, $^4J_{7,5} = 1.6$ Hz), 7.76–7.83 (m, 8 H, H-3, H-21), 8.21 (d, 4 H, H-4, $^3J_{4,3} = 9.2$ Hz), 8.27 (ddd, 4 H, H-20, $^3J_{20,21} = 7.8$ Hz, $^3J_{20,19} = 7.8$ Hz, $^4J_{20,22} = 1.7$ Hz), 8.34 (d, 4 H, H-5, $^4J_{5,7} = 1.6$ Hz), 8.42 (dd, 4 H, H-14, $^3J_{14,15} = 8.4$ Hz, $^4J_{14,17} = 2.1$ Hz), 8.68–8.74 (m, 8 H, H-15, H-19), 8.94 (d, 4 H, H-22, $^3J_{22,21}$ = failed resolution), 9.07 (d, 4 H, H-17, $^4J_{17,14} = 2.1$ Hz) ppm; ^{13}C NMR (100.6 MHz, DMF-*d*₇) δ 55.4 (C-24), 85.5 (C-12), 94.6 (C-23), 95.4 (C-11), 117.2 (C-6), 117.7 (C-3), 120.0 (C-1), 121.7 (C-13), 122.5 (C-15), 123.2 (C-19), 125.5 (C-8), 126.0 (C-21), 128.6 (C-7), 129.2 (C-10), 130.0 (C-4), 132.5 (C-5), 133.8 (C-9), 139.4 (C-20), 141.1 (C-14), 151.1 (C-16), 151.4 (C-22), 151.6 (C-18), 153.0 (C-17), 154.2 (C-2) ppm; MS (ESI, pos): *m/z* (%) = 839.1 ($\{\text{Ag}_2(\text{M})\text{-1}\}_2^{2+}$, $\{\text{Ag}(\text{M})\text{-1}\}^+$, 100), 753.1 ($\{\text{Na}_2(\text{M})\text{-1}\}_2^{2+}$, $\{\text{Na}(\text{M})\text{-1}\}^+$, 45) 731.2 ($\{(\text{M})\text{-1} + \text{H}\}^+$, 60); CD [λ ($\Delta\epsilon$):] (*M*) = 239 (33.0), 255 (−16.4), 371 (−3.8); (*P*) = 238 (−31.7), 256 (15.2), 367 (3.8).

$\{\text{Cu}_2(\text{M})\text{-1}\}_2(\text{BF}_4)_2/\{\text{Cu}_2(\text{P})\text{-1}\}_2(\text{BF}_4)_2$. MS (ESI, pos): *m/z* (%) = 794.1 ($\{\text{Cu}_2(\text{R}_a)\text{-1}\}_2^{2+}$, 100); CD [λ ($\Delta\epsilon$):] (*M*) = 240 (33.1), 255 (−19.3), 292 (−5.9), 356 (4.7); (*P*) = 239 (−31.4), 255 (18.7), 292 (5.9), 355 (−3.9).

$\{\text{Fe}_2(\text{M})\text{-1}\}_3(\text{BF}_4)_4/\{\text{Fe}_2(\text{P})\text{-1}\}_3(\text{BF}_4)_4$. MS (ESI, pos): *m/z* (%) = 575.9 ($\{\text{Fe}_2(\text{M})\text{-1}\}_3^{4+}$, 100), 774.2 ($\{\text{Fe}_2(\text{M})\text{-1}\}_3 + \text{F}\}^{3+}$, 25); CD [λ ($\Delta\epsilon$):] (*M*) = 241 (53.9), 258 (−34.7), 313 (−3.2), 411 (−3.0); (*P*) = 240 (−48.6), 257 (34.9), 311 (4.5) 414 (4.4).

$\{\text{Zn}_2(\text{M})\text{-1}\}_2(\text{BF}_4)_4/\{\text{Zn}_2(\text{M})\text{-1}\}_3(\text{BF}_4)_4 // \{\text{Zn}_2(\text{P})\text{-1}\}_2(\text{BF}_4)_4/\{\text{Zn}_2(\text{P})\text{-1}\}_3(\text{BF}_4)_4$. MS (ESI, pos): *m/z* (%) = 580.9 ($\{\text{Zn}_2(\text{M})\text{-1}\}_3^{4+}$, 100), 397.1 ($\{\text{Zn}_2(\text{M})\text{-1}\}_2^{4+}$, $\{\text{Zn}(\text{M})\text{-1}\}^{2+}$, 60), 976.7 ($\{\text{Zn}_2(\text{M})\text{-1}\}_3 + \text{F}\}^{3+}$, 30).

$\{\text{Ag}_2(\text{M})\text{-2}\}_2(\text{BF}_4)_2/\{\text{Ag}_2(\text{P})\text{-2}\}_2(\text{BF}_4)_2$. ^1H NMR (400 MHz, DMF-*d*₇) δ 3.18 (s, 12 H, H-31), 5.19 (d, 4 H, H-30, $^2J_{30,30'} = -7.0$ Hz), 5.25 (d, 4 H, H-27', $^2J_{30',30} = -7.0$ Hz), 7.11 (d, 4 H, H-8, $^3J_{8,7} = 8.7$ Hz), 7.41 (d, 4 H, H-7, $^3J_{7,8} = 8.7$ Hz), 7.49–7.60 (m, 12 H, H-25, H-26), 7.80 (d, 4 H, H-3, $^3J_{3,4} = 9.3$ Hz), 7.90 (d, 8 H, H-24, $^3J_{24,25} = 7.5$ Hz), 8.20 (d, 4 H, H-4, $^3J_{4,3} = 9.3$ Hz), 8.33 (s, 4 H, H-5), 8.43 (d, 4H, H-14, $^3J_{14,15} = 8.2$ Hz), 8.59 (d, 4 H, H-20, $^3J_{20,19} = 8.4$ Hz), 8.74–8.82 (m, 8 H, H-15, H-19), 9.10 (s, 4 H, H-17), 9.34 (s, 4 H, H-22) ppm; ^{13}C NMR (100.6 MHz, DMF-*d*₇) δ 55.4 (C-28), 85.6 (C-12), 94.6 (C-27), 95.5 (C-11), 117.2 (C-6), 117.7 (C-3), 120.0 (C-1), 121.7 (C-13), 122.5 (C-15), 123.2 (C-19), 125.5 (C-8), 127.2 (C-24), 128.6 (C-7), 129.1 (C-26), 129.2 (C-10), 129.4 (C-25), 130.0 (C-4), 132.5 (C-5), 133.8 (C-9), 136.0 (C-23), 136.9 (C-20), 137.8 (C-21), 141.1 (C-14), 149.5 (C-22), 150.3 (C-18), 150.8 (C-16), 153.1 (C-17), 154.2 (C-2) ppm; MS (ESI, pos): *m/z* (%) = 991.2 ($\{\text{Ag}_2(\text{M})\text{-2}\}_2^{2+}$, $\{\text{Ag}(\text{M})\text{-2}\}^+$, 95), 905.2 ($\{\text{Na}_2(\text{M})\text{-2}\}_2^{2+}$, $\{\text{Na}(\text{M})\text{-2}\}^+$, 45), 442.1 ($\{(\text{M})\text{-2} + 2\text{H}\}^{2+}$, 50), 883.3 ($\{(\text{M})\text{-2} + \text{H}\}^+$, 100); CD [λ ($\Delta\epsilon$):] (*M*) = 232 (34.5), 258 (−12.8), 374 (−7.6); (*P*) = 233 (−32.4), 258 (12.0), 373 (7.9).

$\{\text{Cu}_2(\text{M})\text{-2}\}_2(\text{BF}_4)_2/\{\text{Cu}_2(\text{P})\text{-2}\}_2(\text{BF}_4)_2$. MS (ESI, pos): *m/z* (%) = 946.2 ($\{\text{Cu}_2(\text{M})\text{-2}\}_2^{2+}$, 100); CD [λ ($\Delta\epsilon$):] (*M*) = 233 (37.5), 255 (−17.7), 357 (4.9), 396 (−6.8); (*P*) = 234 (−33.0), 257 (14.2), 357 (−3.7), 395 (6.5).

$\{\text{Fe}_2(\text{M})\text{-2}\}_3(\text{BF}_4)_4/\{\text{Fe}_2(\text{P})\text{-2}\}_3(\text{BF}_4)_4$. MS (ESI, pos): *m/z* (%) = 689.9 ($\{\text{Fe}_2(\text{M})\text{-2}\}_3^{4+}$, 100), 926.6 ($\{\text{Fe}_2(\text{M})\text{-2}\}_3 + \text{F}\}^{3+}$, 30);

CD [λ ($\Delta\epsilon$):] (*M*) = 235 (52.5), 260 (−32.9), 324 (−9.9); (*P*) = 235 (−48.5), 259 (29.9), 324 (8.9).

$\{\text{Zn}_2(\text{M})\text{-2}\}_2(\text{BF}_4)_4/\{\text{Zn}_2(\text{M})\text{-2}\}_3(\text{BF}_4)_4 // \{\text{Zn}_2(\text{P})\text{-2}\}_2(\text{BF}_4)_4/\{\text{Zn}_2(\text{P})\text{-2}\}_3(\text{BF}_4)_4$. MS (ESI, pos): *m/z* (%) = 694.9 ($\{\text{Zn}_2(\text{M})\text{-2}\}_3^{4+}$, 90), 474.1 ($\{\text{Zn}_2(\text{M})\text{-2}\}_2^{4+}$, $\{\text{Zn}(\text{M})\text{-2}\}^{2+}$, 100), 915.7 ($\{\text{Zn}_2(\text{M})\text{-2}\}_4^{4+}$, 25), 932.2 ($\{\text{Zn}_2(\text{M})\text{-2}\}_3 + \text{F}\}^{3+}$, 25).

$\{\text{Ag}_2(\text{M})\text{-3}\}_2(\text{BF}_4)_2/\{\text{Ag}_2(\text{P})\text{-3}\}_2(\text{BF}_4)_2$. ^1H NMR (400 MHz, DMF-*d*₇) δ 0.86 (t, 12H, H-29, $^3J_{29,28} = 6.9$ Hz), 1.23–1.39 (m, 32H, H-25, H-26, H-27, H-28), 1.66–1.73 (m, 8H, H-24), 2.76–2.81 (m, 8H, H-23), 3.17 (s, 12H, H-31), 5.18 (d, 4H, H-30, $^2J_{30,30'} = -6.9$ Hz), 5.25 (d, 4H, H-30', $^2J_{30',30} = -6.9$ Hz), 7.11 (d, 4H, H-8, $^3J_{8,7} = 8.9$ Hz), 7.42 (dd, 4H, H-7, $^3J_{7,8} = 8.9$ Hz, $^4J_{7,5} = 1.5$ Hz), 7.80 (d, 4H, H-3, $^3J_{3,4} = 9.2$ Hz), 8.15 (dd, 4H, H-20, $^3J_{20,19} = 8.5$ Hz, $^4J_{20,22} = 2.0$ Hz), 8.20 (d, 4H, H-4, $^3J_{4,3} = 9.2$ Hz), 8.33 (d, 4H, H-5, $^4J_{5,7} = 1.5$ Hz), 8.39 (dd, 4H, H-14, $^3J_{14,15} = 8.4$ Hz, $^4J_{14,17} = 2.0$ Hz), 8.63 (d, 4H, H-19, $^3J_{19,20} = 8.5$ Hz), 8.70 (d, 4H, H-15, $^3J_{15,14} = 8.4$ Hz), 8.79 (d, 4H, H-22, $^4J_{22,20} = 2.0$ Hz), 9.04 (d, 4H, H-17, $^4J_{17,14} = 2.0$ Hz) ppm; ^{13}C NMR (100.6 MHz, DMF-*d*₇) δ 13.6 (C-29), 22.4 (C-28), (30.90, 30.91) (C-24, C-26)*, 31.6 (C-27)*, 32.2 (C-23), 55.4 (C-31), 85.6 (C-12), 94.6 (C-30), 95.2 (C-11), 117.2 (C-6), 117.7 (C-3), 120.0 (C-1), 121.4 (C-13), 122.1 (C-15), 122.8 (C-19), 125.5 (C-8), 128.6 (C-7), 129.3 (C-10), 130.0 (C-4), 132.4 (C-5), 133.8 (C-9), 139.0 (C-20), 141.0 (C-14, C-21), 149.5 (C-18), 151.3 (C-16, C-22), 152.9 (C-17), 154.1 (C-2) ppm, (C-25) not found; (* = signal assignments might be interchanged); MS (ESI, pos): *m/z* (%) = 1035.3 ($\{\text{Ag}_2(\text{P})\text{-3}\}_2^{2+}$, $\{\text{Ag}(\text{P})\text{-3}\}^+$, 100), 518.2 ($\{\text{Ag}(\text{P})\text{-3} + \text{H}\}^{2+}$, 35), 464.2 ($\{(\text{P})\text{-3} + 2\text{H}\}^{2+}$, 35); CD [λ ($\Delta\epsilon$):] (*M*) = 240 (32.2), 255 (−19.1), 373 (−5.4); (*P*) = 239 (−29.4), 256 (18.5), 372 (5.1).

$\{\text{Cu}_2(\text{M})\text{-3}\}_2(\text{BF}_4)_2/\{\text{Cu}_2(\text{P})\text{-3}\}_2(\text{BF}_4)_2$. MS (ESI, pos): *m/z* (%) = 990.4 ($\{\text{Cu}_2(\text{P})\text{-3}\}_2^{2+}$, 100); CD [λ ($\Delta\epsilon$):] (*M*) = 241 (29.4), 254 (−22.1), 294 (−5.5), 356 (5.7); (*P*) = 240 (−28.2), 254 (21.4), 294 (4.6), 355 (−4.2).

$\{\text{Fe}_2(\text{M})\text{-3}\}_3(\text{BF}_4)_4/\{\text{Fe}_2(\text{P})\text{-3}\}_3(\text{BF}_4)_4$. MS (ESI, pos): *m/z* (%) = 723.3 ($\{\text{Fe}_2(\text{P})\text{-3}\}_3^{4+}$, 100), 970.7 ($\{\text{Fe}_2(\text{P})\text{-3}\}_3 + \text{F}\}^{3+}$, 20); CD [λ ($\Delta\epsilon$):] (*M*) = 239 (55.1), 257 (−47.3), 315 (−7.0), 410 (−5.4); (*P*) = 241 (−46.2), 257 (41.1), 316 (8.5), 409 (4.1).

$\{\text{Zn}_2(\text{M})\text{-3}\}_2(\text{BF}_4)_4/\{\text{Zn}_2(\text{M})\text{-3}\}_3(\text{BF}_4)_4 // \{\text{Zn}_2(\text{P})\text{-3}\}_2(\text{BF}_4)_4/\{\text{Zn}_2(\text{P})\text{-3}\}_3(\text{BF}_4)_4$. MS (ESI, pos): *m/z* (%) = 728.0 ($\{\text{Zn}_2(\text{P})\text{-3}\}_3^{4+}$, 100), 496.2 ($\{\text{Zn}_2(\text{P})\text{-3}\}_2^{4+}$, $\{\text{Zn}(\text{P})\text{-3}\}^{2+}$, 50), 976.7 ($\{\text{Zn}_2(\text{P})\text{-3}\}_3 + \text{F}\}^{3+}$, 25).

Acknowledgment. Dedicated to Dr. Julius Rebek, Jr. on the occasion of his 65th birthday. Financial support of this work from the Deutsche Forschungsgemeinschaft (SFB 624) is gratefully acknowledged.

Supporting Information Available: Spectroscopic data for the ligands 1–3 and their metal complexes; BLYP-optimized structures and energies of the Cu(I), Ag(I), and Fe(II) complexes. This material is available free of charge via the Internet at <http://pubs.acs.org>.

JA807780J